0026-895X/06/7002-571–578$20.00
MOLECULAR PHARMACOLOGY
Vol. 70, No. 2
24075/3130846
Mol Pharmacol 70:571–578, 2006
Printed in U.S.A.

Mapping Residues in the Ligand-Binding Domain of the 5-HT_3 Receptor onto *d*-Tubocurarine Structure

Dong Yan, Julia K. Meyer, and Michael M. White

Department of Pharmacology and Physiology, Drexel University College of Medicine, Philadelphia, Pennsylvania

Received March 3, 2006; accepted May 23, 2006

ABSTRACT

The serotonin 5-HT_3 receptor (5-HT_3R) is a member of the cys-loop ligand-gated ion channel family. We have used the combination of site-directed mutagenesis, homology modeling of the 5-HT_3R extracellular domain, and ligand docking simulations as a way to map the architecture of the 5-HT_3R ligand binding domain. Mutation of Phe226 in loop C of the binding site to tyrosine (F226Y) has no effect on the apparent affinity of the competitive antagonist *d*-tubocurarine (*d*TC) for the receptor. On the other hand, replacement of Asn128 in loop A of the binding site with alanine (N128A) increases the apparent affinity of *d*TC by approximately 10-fold. Double-mutant cycle analysis employing a panel of *d*TC analogs with substitutions at various positions to identify specific points of interactions between the *d*TC analogs and Asn128 suggests that Asn128 makes a direct interaction with the 2′N of *d*TC. Molecular modeling of the 5-HT_3R extracellular domain using the antagonist-bound conformation of the *Aplysia californica* acetylcholine binding protein as a template followed by ligand docking simulations produces two classes of structures of the 5-HT_3R/*d*TC complex; only one of these has the 2′N of *d*TC positioned at Asn128 and thus is consistent with the data from this study and previously published data. The use of the rigid *d*TC analogs as "molecular rulers" in conjunction with double-mutant cycle analysis of mutant receptors can allow the spatial mapping of the position of various residues in the ligand-binding site.

The serotonin type 3 receptor (5-HT_3R) is a member of the cys-loop ligand-gated ion channel gene family, which includes the muscle and neuronal nicotinic acetylcholine receptors (AChR), the glycine receptor, and the GABA type A receptor (Connolly and Wafford, 2004; Lester et al., 2004). Two different subunits, termed 5-HT_{3A} and 5-HT_{3B}, have been shown to be present in functional 5-HT_3Rs (Reeves and Lummis, 2002). In addition, several other putative 5-HT_3R genes have been described, but whether or not they play a role in 5-HT_3R-mediated processes is unknown at present (Karnovsky et al., 2003). The 5-HT_{3A} subunit alone can form functional receptors with the appropriate pharmacological properties when expressed in *Xenopus laevis* oocytes or mammalian cells. However, receptors comprising only the 5-HT_{3A} subunit have single-channel conductances in the subpicosiemens range, whereas those containing both the 5-HT_{3A} and 5-HT_{3B} subunits have conductances in the 10- to 30-pS range (Davies et al., 1999; Dubin et al., 1999; Hanna et al., 2000), similar to that observed in neurons from the peripheral nervous system (Derkach et al., 1989; Yang et al., 1992). The reduction in single-channel conductance of homomeric 5-HT_{3A}Rs is now know to be due to the presence of three arginine residues in the cytoplasmic domain, and removal of these three positive charges results in a single-channel conductance on the order of 25 pS (Kelley et al., 2003). Analysis of the expression patterns of the 5-HT_{3A} and 5-HT_{3B} subunits has led to the suggestion that the bulk of the 5-HT_3Rs in the central nervous system are 5-HT_{3A} homomers, whereas those in the peripheral nervous system are a mixture of 5-HT_{3A} homomers and 5-HT_{3A}/5-HT_{3B} heteromers (Morales and Wang, 2002). However, despite the differences in the single-channel properties of the two types of receptors, they have essentially identical ligand-binding properties (Brady et al., 2001). Thus, homomeric 5-HT_{3A}Rs should be an appropriate model for the structure of the ligand-binding domain of native 5-HT_3Rs, regardless of whether they are 5-HT_{3A} homomers or 5-HT_{3A}/5-HT_{3B} heteromers.

Structural models for the 5-HT_3R have recently been developed by several groups (Maksay et al., 2003; Reeves et al., 2003; Yan and White, 2005), taking advantage of the homology between the various members of the ligand-gated ion channel family and a soluble ACh-binding protein (AChBP) isolated from the snail *Lymnaea stagnalis*, for which the

This work was supported by a grant from the American Heart Association Pennsylvania-Delaware Affiliate.
Article, publication date, and citation information can be found at http://molpharm.aspetjournals.org.
doi:10.1124/mol.106.024075.

ABBREVIATIONS: 5-HT_3R, serotonin type 3 receptor; AChR, nicotinic acetylcholine receptors; *d*TC, *d*-tubocurarine; WT, wild type; AChBP, acetylcholine binding protein.

structure has been solved to atomic resolution (Brejc et al., 2001; Smit et al., 2001). In these various models, ligand-docking simulations produce several orientations of agonists (Reeves et al., 2003) or antagonists (Maksay et al., 2003; Thompson et al., 2005; Yan and White, 2005) in the binding site, and the authors used data obtained from mutagenesis studies to evaluate models for consistency with experimental data to select feasible structural models for receptor-ligand interactions. In some cases, the investigators correlated the effects of a number of previously studied mutations in the receptor on ligand affinity with expectations derived from the structural models (Maksay et al., 2003; Reeves et al., 2003), whereas in others, mutations designed after the model was created were used to test the model (Thompson et al., 2005; Yan and White, 2005). Although most of these studies involved monitoring the effect of changing only the receptor, we combined the approach of introducing mutations in the receptor itself with alterations in ligand structure to more fully probe ligand-receptor interactions via double-mutant cycle analysis (Yan and White, 2005). With this approach, we were able to map different portions of the antagonist granisetron onto different regions of the ligand-binding site, allowing an unambiguous discrimination among different models with different orientations of the antagonist granisetron in the binding site. Assuming that one can introduce structural changes in both the receptor and the ligand, the application of double-mutant cycle analysis represents a powerful for probing ligand-receptor interactions.

A limiting factor in the application of double-mutant cycle analysis to nonpeptidic ligands is the availability of a panel of ligands with a number of defined small changes in structure. One ligand that can be altered in a number of ways is *d*-tubocurarine (*d*TC). Although well known as a neuromuscular blocking agent (Bernard and Pelouze, 1850) and nicotinic AChR competitive antagonist (Jenkinson, 1960), it also has nanomolar affinity for the murine 5-HT_3R (Lummis et al., 1990; Peters et al., 1990; Newberry et al., 1991). Using a series of *d*TC analogs originally designed for analysis of *d*TC-AChR interactions (Pedersen and Papineni, 1995; Papineni and Pedersen, 1997), we demonstrated that the same regions of *d*TC that were important for high-affinity binding to the AChR were also important for binding to the 5-HT_3R (Yan et al., 1998), reinforcing the notion that the ligand-binding domains of the AChR and the 5-HT_3R share common features. In a subsequent study, we examined the effects of two mutations known to affect antagonist binding to the 5-HT_3R (W90F and R92A) on the affinity of a series of *d*TC analogs (Yan and White, 2002). We found that the W90F mutation decreased *d*TC affinity, whereas the R92A mutation increased *d*TC affinity, and that the alteration in affinity was more or less equal for all analogs examined. This led us to conclude that although these two residues might affect the overall properties of the binding site, they did not make a direct physical contact with those portions of *d*TC that we could modify.

In this study, we have examined the effects of two additional mutations in residues near granisetron in our model (N128A and F226Y) on the interaction of *d*TC with the 5-HT_3R. We find that although the F226Y mutation has no effect on the affinity of any of the analogs tested, the N128A mutation increases the affinity of some (but not all) of the analogs. The differential effect of this mutation on analog affinity allows us to map the interaction of Asn128 to a particular region of *d*TC. Taken in conjunction with molecular modeling studies and the results of our previous study, these data allow us to determine the orientation of *d*TC in the ligand-binding domain and map different regions of the antagonist onto residues in the ligand-binding domain.

Materials and Methods

Molecular Biology and Transfection. A full-length cDNA clone corresponding to the 5-$HT_{3A(b)}$ form (Hope et al., 1993) of the receptor was isolated from a neuroblastoma N1E-115 cell line cDNA library as described previously (Yan et al., 1999) and subcloned into vector pCI (Promega, Madison, WI). Site-directed mutagenesis was carried out using the QuikChange system (Stratagene, La Jolla, CA) as described previously (Yan et al., 1999). The nomenclature used to describe mutants is amino acid in wild-type/position/substitution (e.g., N128A). Because the amino terminus of the mature 5-HT_{3A} subunit is unknown, the amino acid numbering system used here includes the signal sequence and starts from the initial methionine. Cultures of tsA201 cells, a derivative of the widely used human embryonic kidney 293 cell line, were maintained in Dulbecco's modified Eagle's medium containing 10% fetal bovine serum, 100 units/ml penicillin, and 100 units/ml streptomycin. Cultures at 30 to 40% confluence were transfected with 6 μg of receptor cDNA per 100-mm dish using the Fugene transfection reagent (Roche Diagnostics, Indianapolis, IN). Maximal expression was obtained 36 to 72 h after transfection.

Ligand Binding Assays. Transfected cells were scraped from dishes, washed three times with phosphate-buffered saline, and resuspended and homogenized in 2.5 ml of 154 mM NaCl, 50 mM Tris-HCl, pH 7.4, per 100 mm dish. The homogenate was then used in binding assays or frozen until needed. We observed no change in either ligand affinity or B_{max} values after freezing.

Membranes were incubated for 2 h at 37° in a total volume of 0.5 ml of 154 mM NaCl and 50 mM Tris-HCl, pH 7.4, containing the appropriate concentrations of the competing unlabeled ligand and radioligand ([^{3}H]granisetron, 85 Ci/mmol; PerkinElmer Life and Analytical Sciences, Boston, MA). Binding was terminated by rapid vacuum filtration onto GF/B filters that had been pretreated with 50 mM Tris-HCl, pH 7.4, and 0.2% polyethylenimine, and the filters were washed with 10 ml of ice-cold 50 mM Tris-HCl, pH 7.4, per sample. Nonspecific binding was defined as that binding not displaced by 100 μM *m*-chlorophenyl biguanide. IC_{50} values for the various *d*TC analogs were determined by fitting the data to the following equation, using a Levenberg-Marquardt algorithm in a commercially available software package (Igor Pro; WaveMetrics, Oswego, OR): $\theta = [1 + ([I]/IC_{50})^{n_H}]^{-1}$, where θ is the fractional amount of [^{3}H]granisetron bound in the presence of the antagonist at concentration [I] compared with that in the absence of antagonist, IC_{50} is the concentration of antagonist at which $\theta = 0.5$, and n_H is the apparent Hill coefficient. K_i values were calculated from the IC_{50} values and the K_d for [^{3}H]granisetron using the Cheng-Prusoff relation (Cheng and Prusoff, 1973): $K_i = IC_{50}/[1 + ([L]/K_d)]$, where [L] is the concentration of [^{3}H]granisetron used to determine the IC_{50} value in the experiment and K_d is the dissociation constant for [^{3}H]granisetron. For the Cheng-Prusoff relation to be applicable, the Hill coefficient for the IC_{50} curve must be equal to 1. In our experiments, all Hill coefficients were not statistically different from unity at a 95% confidence level (data not shown). In this study, all experiments were carried out with a [^{3}H]granisetron concentration equal to its experimentally determined dissociation constant for the particular receptor (WT, 3.0 nM; N128A, 1.7 nM; F226Y, 1.6 nM), meaning that the measured IC_{50} values were twice the K_i.

***d*-Tubocurarine Analogs.** The structures of the *d*-tubocurarine analogs used in this study are shown in Fig. 1. Two of the compounds were obtained commercially [*d*-tubocurarine (Sigma, St. Louis, MO)

and metocurine (Diosynth, Inc., Chicago, IL)], and the others were obtained from Dr. Steen Pedersen of Baylor University College of Medicine (Houston, TX) (Pedersen and Papineni, 1995; Papineni and Pedersen, 1997). Purity of all compounds was checked by high-performance liquid chromatography both before use and after prolonged incubation with the assay buffers.

Molecular Modeling and Ligand Docking. A structural model of the extracellular domain of the mouse 5HT$_{3A}$R was generated using version 7.7 of the program MODELLER (Sali and Blundell, 1993), using the X-ray structure of both the *Lymnaea stagnalis* AChBP [Protein Data Bank ID 1I9B (Brejc et al., 2001)] and the methllycaconitine-bound form of the *Aplysia californica* AChBP [Protein Data Bank ID 2BYR, (Hansen et al., 2005)] as templates as described previously (Yan and White, 2005).

d-Tubocurarine was docked to each binding site in the chosen model using Autodock 3.0 (Morris et al., 1998). Solvation parameters were added to the protein coordinate file and the ligand torsions were defined using the Addsol and Autotors utilities, respectively, in Autodock 3.0. Gasteiger-Marsili charges were applied to ligands before docking (Gasteiger and Marsili, 1980), which use the united atom representation for nonpolar hydrogens. The docking was performed with the initial population size set to 100 with 100 independent runs using otherwise default parameters in the standard protocol on a 30 × 30 × 40-Å grid with spacing of 0.375 Å. The size of the grid gives sufficient freedom for the ligands to be docked in all possible orientations but does not permit them move outside of the binding site. In addition to returning the docked structure, AutoDock also calculates an affinity constant for each ligand-receptor configuration. AutoDock allows flexibility in the ligand, and it has been shown that conformations of ligands docked in a binding site with AutoDock agree with bound conformations in crystal structures of ligand-protein complexes (Osterberg et al., 2002). Images were produced using the UCSF Chimera package (Pettersen et al., 2004) from the Computer Graphics Laboratory, University of California, San Francisco (supported by National Institutes of Health grant P41-RR01081).

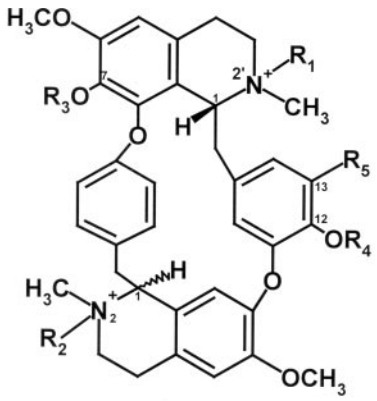

R_1	R_2	R_3	R_4	R_5	Stereo Isomer 1	Stereo Isomer 1'	NAME
CH_3	H	H	H	H	S	R	*d*-Tubocurarine
H	H	H	H	H	S	R	Tubocurine
CH_3	CH_3	H	H	H	S	R	Chondocurarine
H	H	CH_3	CH_3	H	S	R	O,O-dimethyl-tubocurine
CH_3	CH_3	CH_3	H	H	S	R	7'-O-methyl-chondocurarine
CH_3	CH_3	H	CH_3	H	S	R	12'-O-methyl-chondocurarine
CH_3	CH_3	CH_3	CH_3	H	S	R	Metocurine
CH_3	H	H	H	I	S	R	Iodo-*d*-tubocurarine
CH_3	H	H	H	Br	S	R	Bromo-*d*-tubocurarine
CH_3	H	H	H	SO_3^-	S	R	Sulfo-*d*-tubocurarine
H	H	H	H	H	R	R	*l*-Bebeerine

Fig. 1. *d*-Tubocurarine analogs used in this study. Note the location of the 2′N in the upper right-hand portion and the 2N in the lower left-hand portion of *d*TC, respectively.

Results

We focused on two amino acid residues (Asn128 and Phe226) in the 5-HT$_{3A}$R that were predicted to be near granisetron in our model of the granisetron-5-HT$_{3A}$R complex (Yan and White, 2005). Neither mutation had a statistically significant effect on the affinity of granisetron, in agreement with a previous report (Thompson et al., 2005). We obtained estimates for the affinity of a number of *d*TC analogs (Fig. 1) with wild-type, N128A, and F226Y mutant 5-HT$_3$Rs using competitive inhibition of the binding of the antagonist [^{3}H]granisetron (Table 1). Although the F226Y mutation had no effect on the affinity for all five compounds tested, the N128A mutation did have statistically significant effects on the affinity of some, but not all, of the ligands. Figure 2 shows the inhibition of [^{3}H]granisetron binding to wild-type and N128A receptors by *d*TC (top) and tubocurine (bottom). The N128A mutation increases the apparent affinity of *d*TC for the receptor approximately 6-fold, whereas it has no effect on the affinity for tubocurine. These two compounds differ only by the presence of an additional methyl group on the 2′N of the molecule, converting the tertiary amine of tubocurine to a quaternary amine in *d*TC. The differential sensitivity suggests that Asn128 interacts with the 2′N of the antagonist. Examination of the effect of the mutation on other analogs indicates that the mutation increases the affinity of those analogs with a quaternary amine at the 2′N position, but has no effect on the affinity of the analogs that have a tertiary amine at the 2′N position.

To explore this further, we analyzed the effects of the N128A mutation on a number of analogs using double-mutant cycle analysis. Double-mutant cycle analysis (Carter et al., 1984) can be used to determine whether or not a particular residue interacts with a particular portion of a ligand. The underlying logic of this approach is that if residue *x* in the binding site interacts with residue *y* on the ligand, then the effect of mutating *x* should depend upon whether residue *y* in the ligand is changed or not. An interaction parameter, Ω, is calculated from the K_d or K_i values as $(K_{W,L1}/K_{W,L2})/(K_{M,L1}/K_{M,L2})$, where the subscripts indicate the following: *W* for wild-type receptor, *M* for mutant receptor, and *L1* and *L2* for the two ligands being compared. An Ω value significantly different from 1 indicates an interaction between the functional group on the ligand and the residue in question on the receptor. Although initially used for analysis of the interaction of peptide toxins with K^+ channels (Hildago and MacKinnon, 1995), this approach has also been applied to identify points of contact between AChRs and peptide toxins (Malany et al., 2000), AChRs and *d*-tubocurarine analogs (Willcockson et al., 2002) and granisetron and the 5-HT$_3$R (Yan and White, 2005).

Figure 3 shows two double-mutant cycles constructed for the interaction of *d*TC analogs with the receptor. The right side of the figure shows the dTC/tubocurine/WT/N128A cycle, in which the difference in the ligands is only at the 2′N; *d*TC has a quaternary nitrogen at 2′N and tubocurine has a tertiary nitrogen at this position. In this cycle, an Ω value of 5.5 ± 1.2 is obtained, consistent with the N128A mutation affecting a direct interaction between the 2′N of *d*TC and Asn128 of the receptor. The left side of the figure shows the dTC/chondocurarine/WT/N128A cycle. These two ligands differ at the 2N position; chondocurarine has a quaternary

nitrogen at this position and *d*TC has a tertiary nitrogen. The Ω value for this cycle is 1.4 ± 0.2, suggesting that there is no direct interaction between Asn128 and the 2N of *d*TC.

Table 2 shows the Ω values determined form a total of seven double-mutant cycles. In all cases in which there is a difference at the 2′N position between the two ligands in the pair (*d*TC/tubocurine, *d*TC/metocurine, *d*TC/*O*,*O*-dimethyltubocurine, metocurine/tubocurine), an Ω value significantly different from 1 is obtained, whereas for those cycles in which there is no difference at the 2′N position (but there are differences at other positions), the Ω value is close to 1.

To gain some insight into potential interactions between *d*TC and Asn128 and other residues in the 5-HT_3R ligand-binding site, we carried out ligand-docking simulations between *d*TC and the 5-HT_3R ligand-binding domain using a model for the receptor created by homology modeling with the *L. stagnalis* AChBP as the template. We had previously used this model of the ligand-binding domain in our analysis of granisetron/5-HT_3R interactions. Analysis of the results of docking *d*TC with this model showed that in contrast to granisetron, *d*TC could not fit into the binding site as a high-affinity complex (data not shown). Analysis of the structure of the related *A. californica* AChBP in the apo, agonist-bound, and antagonist-bound states has demonstrated that loop C is in different positions depending upon what is bound to the protein (Celie et al., 2005; Hansen et al., 2005). When agonists are bound to the protein, loop C closes down on the agonist; in the apo or antagonist-bound form, the loop rotates outward like a paddle, with the tip of the loop moving 7 to 11 Å away from the bulk of the AChBP. With a model derived from the agonist-bound conformation (i.e., the *L. stagnalis* AChBP structure), *d*TC is presumably too large to easily enter the site with the loop C covering the entrance, whereas it can do so in models derived from the more open apo or antagonist-bound conformation.

Two main clusters of dTC/5-HT_3R complexes were obtained from the modeling runs using the model derived from the methyllycaconitine-bound form of the *A. californica* AChBP. Figure 4 shows representative complexes from each cluster. The figure shows *d*TC and four residues in the bind-

TABLE 1

Affinity of *d*-tubocurarine analogs for mutant and wild-type 5-HT_3Rs

Estimates of pK_i values (± S.D.) were calculated from experimentally determined pIC_{50} values for the inhibition of [^{3}H]granisetron binding to wild-type or mutant receptors as described under *Materials and Methods*. Errors represent the error determined by the Levenberg-Marquardt regression routine used in the fitting.

Ligand	pK_i		
	WT	N128A	F226Y
d-Tubocurarine	6.93 ± 0.05	7.73 ± 0.04*	6.98 ± 0.14
Tubocurine	7.03 ± 0.05	7.08 ± 0.05	7.05 ± 0.12
Chondocurarine	6.99 ± 0.01	7.93 ± 0.03*	7.01 ± 0.08
Metocurine	5.52 ± 0.02	6.13 ± 0.02*	5.64 ± 0.08
O,*O*-DMTC	5.73 ± 0.06	5.57 ± 0.03	5.55 ± 0.08

* Statistically different from wild-type at a 95% confidence level using Student's *t* test.

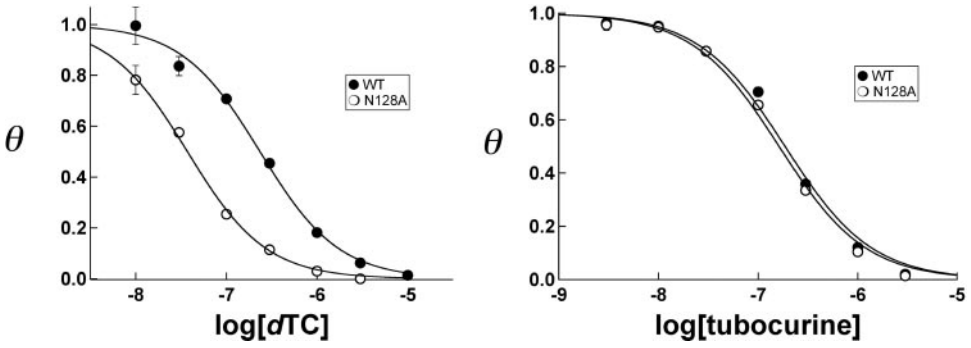

Fig. 2. Effects of N128A mutation on *d*-tubocurarine and tubocurine affinity. The concentration dependences of inhibition of [^{3}H] granisetron binding by *d*TC or tubocurine to wild-type (○) and N128A (●) 5-HT_3Rs are shown. Each data point represents the mean ± S.E.M. of 3 determinations. The solid curves are drawn using IC_{50} values of 236 nM (WT, *d*TC), 40 nM (N128A, *d*TC), 186 nM (WT, tubocurine), and 162 nM (N128A, tubocurine). Note that the N128A mutation increases *d*TC affinity but has no effect on tubocurine affinity.

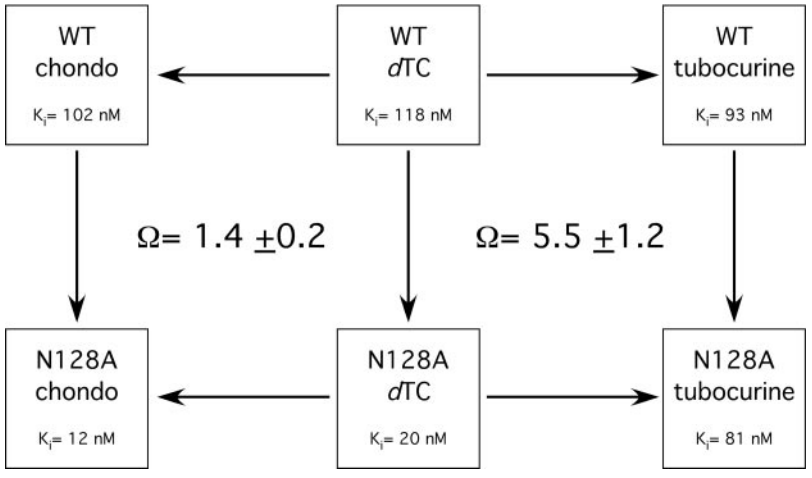

Fig. 3. Double-mutant cycles for WT and N128A receptors and *d*-tubocurarine, tubocurine, and chondocurarine. The interaction coefficient, Ω, for each combination of the receptors (WT, N128A) and ligands (dTC, tubocurine, chondocurarine) was determined from the K_i values of each ligand for each receptor. The Ω value of 5.5 ± 1.2 for the WT/128A/*d*TC/tubocurine cycle indicates that Asn128 interacts with the 2′N of *d*TC, whereas the Ω value of 1.4 ± 0.2 for the WT/128A/*d*TC/chondocurarine indicates that there is no interaction between the 2N of *d*TC and Asn128.

ing site- two previously shown to be important in 5-HT$_3$R/granisetron interactions [Trp90 and Arg92 (Thompson et al., 2005; Yan and White, 2005)] and the two residues examined in this study (Asn128 and Phe226). In Fig. 4A, the 2N of *d*TC is near Asn128 and the 2′N is near Arg92; in Fig. 4B, the orientation of *d*TC is reversed, with the 2N at Arg92 and the 2′N at Asn128. The vast majority of the high-affinity ligand-receptor models (approximately 90%) were in the orientation shown in Fig. 4A. Examination of the potential interactions in these two models in the context of experimental data can provide useful information concerning the orientation of *d*TC in the 5-HT$_3$R ligand-binding site and identify important interactions that determine affinity of the ligand for the receptor.

Discussion

Delineation of the interactions between a given receptor and its ligands can provide useful information for understanding how ligands can affect receptor function as well as for the synthesis of novel ligands with high affinity and selectivity. We have used a two-pronged approach in which information from mutational analysis of ligand-receptor interactions is combined with molecular modeling studies to more fully examine ligand-receptor interactions than could be done by using either approach by itself. In addition, by varying the structure of both the receptor (by site-directed mutagenesis) and the ligand (such as by using derivatives of *d*TC in this study), we are able to determine which parts of the ligand make direct interactions with specific residues in the receptor.

TABLE 2

Ω Values for various ligand pairings

Ω Values were determined for double-mutant cycles using WT and N128A receptors and the indicated ligand pairs from the K_i values as $\Omega = (K_{W,L1}/K_{W,L2})/(K_{M,L1}/K_{M,L2})$, where W = wild-type receptor, M for mutant receptor, and $L1$ and $L2$ for the two ligands being compared. Error estimates were obtained through analysis of propagation of errors (Ku, 1966).

Ligand pair	Differences	Ω
*d*TC/metocurine	2N, 7, 12	1.5 ± 0.2
*d*TC/tubocurine	2′N	5.5 ± 1.2
*d*TC/*O*,*O*-DMTC	2′N, 7, 12	9.0 ± 1.9
Metocurine/tubocurine	2N, 2′N, 7, 12	3.6 ± 0.7
Metocurine/*O*,*O*-DMTC	2N, 2′N	5.9 ± 1.0
O,*O*-DMTC/tubocurine	7, 12	1.6 ± 0.4
*d*TC/chondocurarine	2N	1.4 ± 0.2

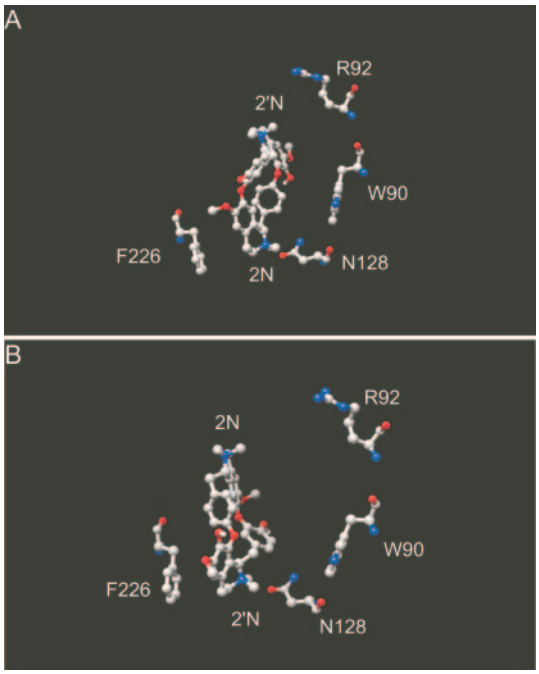

Fig. 4. Representative structural models for *d*TC/5-HT$_3$R complexes. In A, the 2′N of *d*TC is located at Arg92 and the 2N is located at Asn128, whereas in B, the orientation is reversed.

The data presented in Tables 1 and 2 strongly suggest that Asn128 in Loop A of the 5-HT$_3$R makes a direct interaction with the quaternary amine at the 2′N of *d*TC. Replacement of asparagine with alanine at this position (N128A) results in an increase in apparent affinity only for those analogs with a quaternary amine at this position (*d*TC, chondocurarine, metocurine), whereas those analogs with a tertiary amine at this position (tubocurine, *O*,*O*-dimethyltubocurine) are unaffected by this mutation. Double-mutant cycle analysis further bears this out; changes at the 2′N produce a coupling coefficient, Ω, different from 1, whereas cycles with a change at other positions produce Ω values at or near 1.

Molecular modeling of *d*TC/5-HT$_3$R complexes using the *A. californica* AChBP in the antagonist-bound form as a template produces two classes of models. In one, *d*TC is oriented in the ligand-binding site with the 2′N near Arg92 and the 2N near Asn128; in the other, the orientation of *d*TC is flipped. Although the majority of ligand-receptor models were in the former orientation, the mutation data are consistent only with the latter model, in which the 2′N is near Asn128, once again demonstrating the necessity of validating structural models with experimental data specifically designed to test the models.

What type of interaction could Asn128 make with *d*TC at the 2′N position? Because the side chain of Asn128 is uncharged, the increase in affinity after the alanine substitution cannot be due to removal of a charge-charge repulsion. Rather, the increase in affinity is more likely to be due to a steric effect by replacing a larger side chain [asparagine, 117.7 Å^3 (Zamyatnin, 1984)] with a smaller one (alanine, 88.6 Å^3). This could result in a better fit of the quaternary amine of *d*TC at the 2′N position within the binding site, allowing better interactions with other determinants of *d*TC binding. When a smaller tertiary amine is in this position, the steric interaction is less or absent, and reducing the size of the side chain has no effect on affinity.

We previously examined the effects of two different mutations in loop D of the ligand-binding site of the 5-HT$_3$R on the interaction of *d*TC with the receptor (Yan and White, 2002). In that study, replacement of Arg92 with alanine (R92A) increased the affinity of *d*TC for the receptor approximately 8- to 10-fold compared with wild-type receptors and replacement of Trp90 with phenylalanine (W90F) decreased the affinity of *d*TC approximately 4-fold. Examination of the affinities of a number of *d*TC analogs with R92A and W90F receptors led us to conclude that neither residue made a specific interaction with *d*TC. This conclusion was based on the expectation that if specific interactions did occur, we would observe a differential effect of substitutions at one position of *d*TC. However, all analogs showed more or less the same change in affinity as *d*TC. Double-mutant cycle analysis of the interaction of *d*TC analogs with the R92A and W90F mutants is also consistent with this idea, in that all

cycles examined produced Ω values close to 1 (data not shown).

Examination of the *d*TC/5-HT_3R model, which is consistent with the data presented in this study, explains the effects previously reported. In this model, Arg92 is close to the tertiary amine at the 2N position. Removal of the positive charge at Arg92 (R92A) increases *d*TC affinity, which would be consistent with the removal of a charge-charge repulsion between the asparagine and the positively charged amine. All analogs tested have a positive charge at the 2N position, some as a tertiary amine (e.g., tubocurine) and others as a quaternary amine (e.g., chondocurarine). The pK_a of the tertiary amine at the 2N position of *d*TC is on the order of 9.5 or 10 (Barlow, 1982), so both the tertiary and quaternary amines would be positively changed under the conditions employed in this study. Thus, each analog would increase affinity to the same extent because of the loss of the charge-charge repulsion, and we would not have observed any differential effect of various analogs in our previous study because all analogs tested retain the charge at the 2N position.

What about the decrease in affinity observed with the W90F mutation? In the model, Trp90 is positioned somewhat perpendicular to the aromatic ring in *d*TC-containing positions 13 and 12. This could provide an aromatic-aromatic interaction (Burley and Petsko, 1985), which could contribute to the overall binding. We have shown previously that substitutions at the 12 and 13 positions decreased the affinity of *d*TC analogs relative to *d*TC for wild-type, R92A, and W90F receptors (Yan et al., 1998; Yan and White, 2002). *d*TC has a hydrogen at position 13 and a hydroxyl at position 12. Substitutions at either position (methoxy at position 12 and iodine, bromine, or sulfonate at position 13) all increase the size of the substituents on the aromatic ring, possibly creating a steric impediment to the aromatic-aromatic interaction. Replacement of tryptophan with phenylalanine (W90F) may also move the aromatic ring just enough to weaken/eliminate the interaction, resulting in the observed 4-fold decrease in affinity.

We have identified three residues (Trp90, Arg92, and Asn128) as playing important roles in *d*TC/5-HT_3R interactions. The human 5-HT_3R has an approximately 1500-fold lower affinity for *d*TC than does the murine receptor (Bufton et al., 1993; Hope et al., 1996; Yan et al., 1998; Hope et al., 1999). Examination of the sequences of the six binding loops of the murine and human receptors shows that loops A, B, and D are identical in the two species, whereas loops C, E, and F contain some differences between the two species. Trp90 and Arg92 are in loop D, and Asn128 is in loop A, and are conserved between the two species, so they do not play a role in the differential sensitivity between the two species. Phe226 (which does not interact with *d*TC but is presumably in the binding site) is in loop C, but this residue is also conserved between the two species, so it is not responsible for the difference in affinity between the two species. Hope et al. (1999) examined the effects of the species differences in loop C on *d*TC affinity. There are six differences between the murine and the human receptors in this loop and the adjacent sequence. No single amino acid replacement between mouse and human sequences in this region resulted in more than a 9-fold change in affinity. Replacement of all six residues in the murine receptor with the corresponding residues from the human receptor results in an approximately 150-fold decrease in *d*TC affinity, whereas the reciprocal replacements in the human receptor results in an approximately 50-fold increase in *d*TC affinity. Although these results do demonstrate that the differences in the sequences of loop C between the two species are partially responsible for the differences in *d*TC affinity, they account for only some of the differential sensitivity. Examination of the positions of the residues in loop E [His(Arg)145, Arg(Gln)147, with the corresponding human residue in parentheses] and loop F [Ser(Leu)197, Glu(Lys)200, Arg(Lys)202, Lys(Arg)205, Ile(Met)209] that differ between the two species in the model of the *d*TC/5-HT_3R complex used in this study shows that the residues in loop E are far from the docked *d*TC and thus may not contribute to the species difference in dTC affinity, whereas three in loop F (Glu200, Arg202, Lys205) may be close enough to affect *d*TC-receptor interactions. The most significant difference in this region is the replacement of a negatively charged glutamate in the mouse receptor (Glu200) with a positively charged lysine in the human receptor. Charge reversal at this position could affect *d*TC-receptor interaction and may contribute to the observed differences in affinity between the two species. The effect could be due either to the removal of a direct interaction between Glu200 and *d*TC or to an alteration of a structural component of the binding site. In the β-strand conformation of loop F, the side chain of Glu200 would be next to that of the positively charged Arg202in the mouse receptor, perhaps forming a salt bridge that plays a role in the conformation of the binding site. In the human receptor, Glu200 is replaced by a lysine residue and Arg202 is replaced by a lysine residue. In this situation, rather than having a potential salt-bridge pair, the human receptor has two positive resides, which may lead to a charge-charge repulsion and a subsequent alteration of the conformation of the binding site which may result in a lower affinity for *d*TC. Given that the poor structural resolution of loop F in the AChBP (Brejc et al., 2001) and the uncertainty in the exact positions of side chains in any structural models derived from homology considerations, this interpretation is highly speculative and awaits further experimental analysis before any firm conclusions are justified.

There has been one other modeling study on the interaction of *d*TC with the 5-HT_3R (Maksay et al., 2003). These authors used the *L. stagnalis* AChBP as the template for modeling, and a single model for the *d*TC/5-HT_3R complex was presented for the mouse and human receptors. Although it is difficult to discern the detailed structure of the published model, and no information about the predicted affinity of the ligand-receptor complex was presented, it seems to be somewhat similar to the model that we discarded as being inconsistent with our data (i.e., with the 2N near Asn128). However, it must be noted that they used the *Lymnaea* AChBP as the template for modeling, and we were unable to obtain any high-affinity *d*TC/5-HT_3R complexes using models derived from this template. Although the authors considered their model to be consistent with experimental results obtained by other workers, the level of comparison of their model with actual results was somewhat cursory. Until experiments are designed to directly test a given model, one should not put too much credence in a given model.

Two other groups have combined molecular modeling with mutational analysis to examine the interaction of *d*TC with the AChBP and the AChR. In the case of the AChBP, Gao et

al. (2003) concluded that *d*TC bound to the AChBP with the 2′N near (but not immediately adjacent to) Gln55 in loop D (which is homologous to Arg92 in the 5-HT_3R) and the 2N near (but not immediately adjacent to) Tyr89 in loop A (which is homologous to Asn128 in the 5-HT_3R). This model is somewhat similar to the model of Maksay et al. (2003) for the *d*TC/5-HT_3R complex and the model that we discarded based on our double-mutant cycle analysis. Mutational analysis was consistent with this model, but only two analogs (*d*TC and metocurine) were employed in the analysis. Because *d*TC and metocurine differ at three different positions (Fig. 1), Maksay et al. (2003) would not be able to conclusively assign interactions of different portions of *d*TC (or metocurine) within the binding site as would be possible with a larger set of analogs

Using a more complete set of mutations and analogs and double-mutant cycle analysis, Willcockson et al. (2002) examined the interaction of *d*TC with the mouse muscle AChR. Using their experimental data and modeling of the *d*TC-AChR complex with the AChBP as a template, they concluded that the orientation of *d*TC in the complex was such that the 2′N was near αTyr93 of the AChR (homologous to Asn128 in the 5-HT_3R) and the 2N is near γTyr117 (homologous to Gln151 in the 5-HT_3R), similar to the model that is consistent with our experimental data. Exactly why two groups working on very similar proteins should obtain essentially opposite orientations of *d*TC in the binding site is unclear, but given that the model for the *d*TC-AChR complex obtained by Willcoxson et al. (2002) has more rigorous experimental support, we prefer that one. It should be noted that the exact orientation of *d*TC in all of the models is different in each laboratory, and no two models are exactly the same; this is a reflection of the uncertainties of the fine details of molecular modeling.

This study shows the power of double-mutant cycle analysis with small molecule ligands of differing structure to probe ligand-receptor interactions in a way that can map differing portions of the ligand onto specific regions of the receptor. In conjunction with molecular modeling studies, an iterative loop of modeling and experimental testing of models can be created that can accelerate the process of elucidating the three-dimensional architecture of a ligand-binding domain. Inclusion of a wide variety of ligands and mutant receptors should allow the examination of the architecture of the entire ligand-binding domain and thus provide useful information for the design of novel pharmacological agents with both high affinity and high specificity for use as therapeutic agents.

References

Barlow R (1982) The ionization of morphine, hydroxyamphetamine and (+)-tubocurarine chloride and a new method for calculating zwitterion constants. *Br J Pharmacol* **75:**503–512.

Bernard C and Pelouze J (1850) Recherches sur le curare. **31:**533–537.

Brady C, Stanford I, Ali I, Lin L, Williams J, Dubin A, Hope A, and Barnes N (2001) Pharmacological comparison of human homomeric 5-HT_{3A} receptors versus heteromeric 5-$HT_{3A/3B}$ receptors. *Neuropharmacology* **41:**282–284.

Brejc K, van Dijk W, Klaassen R, Schuurmans M, van der Oost J, Smit A, and Sixma T (2001) Crystal structure of an ACh-binding protein reveals the ligand-binding domain of nicotinic receptors. *Nature (Lond)* **411:**269–276.

Bufton K, Steward L, Barber P, and Barnes N (1993) Distribution and characterization of the [^{3}H]granisetron-labelled 5-HT3 receptor in the human forebrain. *Neuropharmacology* **32:**1325–1331.

Burley S and Petsko G (1985) Aromatic-aromatic interaction: a mechanism of protein structure stabilization. *Science (Wash DC)* **229:**23–28.

Carter P, Winter G, Wilkinson A, and Fersht A (1984) The use of double mutants to detect structural changes in the active site of tyrosyl-tRNA synthetase (*Bacillus stearothermophilus*). *Cell* **38:**835–840.

Celie P, Kasheverov I, Mordvintsev D, Hogg R, van Nierop P, van Elk R, van Rossum-Fikkert S, Zhmak M, Bertrand D, Tsetlin V, et al. (2005) Crystal structure of nicotinic acetylcholine receptor homolog AChBP in complex with an α-conotoxin PnIA variant. *Nat Struct Mol Biol* **12:**582–588.

Cheng Y and Prusoff W (1973) Relationship between inhibition constant (K_i) and the concentration of inhibitor which causes 50 percent inhibition (IC_{50}) of an enzymatic reaction. *Biochem Pharmacol* **22:**3099–3108.

Connolly C and Wafford K (2004) The cys-loop superfamily of ligand-gated ion channels: the impact of receptor structure on function. *Biochem Soc Trans* **32:**529–534.

Davies P, Pistis M, Hanna M, Peters J, Lambert J, Hales T, and Kirkness E (1999) The $5HT_{3B}$ subunit is a major determinant of serotonin receptor function. *Nature (Lond)* **397:**359–363.

Derkach V, Suprenant A, and North R (1989) 5-HT_3 receptors are membrane ion channels. *Nature (Lond)* **339:**706–709.

Dubin A, Huvar R, D'Andrea M, Pyati J, Zhu J, Joy K, Wilson S, Galindo J, Glass C, Luo L, et al. (1999) The pharmacological and functional characteristics of the serotonin 5-HT_{3A} receptor are specifically modified by a 5-HT_{3B} receptor subunit. *J Biol Chem* **274:**30799–30810.

Gao F, Bren N, Litle A, Wang H-L, Hansen S, Talley T, Taylor P, and Sine S (2003) Curariform antagonists bind in different orientations to acetylcholine-binding protein. *J Biol Chem* **278:**23020–23026.

Gasteiger J and Marsili M (1980) Iterative partial equalization of orbital electronegativity—a rapid access to atomic charges. *Tetrahedron* **36:**3219–3228.

Hanna M, Davies P, Hales T, and Kirkness E (2000) Evidence for expression of heteromeric serotonin 5-HT_3 receptors in rodents. *J Neurochem* **75:**240–247.

Hansen S, Sulzenbacher G, Huxford T, Marchot P, Taylor P, and Bourne Y (2005) Structures of *Aplysia* AChBP complexes with nicotinic agonists and antagonists reveal distinctive binding interfaces and conformations. *EMBO (Eur Mol Biol Organ) J* **24:**3635–3646.

Hildago P and MacKinnon R (1995) Revealing the architecture of a K^+ channel pore through mutant cycles with a peptide inhibitor. *Science (Wash DC)* **268:**307–310.

Hope A, Belelli D, Mair I, Lambert J, and Peters J (1999) Molecular determinants of (+)-tubocurarine binding at recombinant 5-hydroxytryptamine$_{3A}$ receptor subunits. *Mol Pharmacol* **55:**1037–1043.

Hope A, Downie D, Sutherland L, Lambert J, Peters J, and Burchell B (1993) Cloning and functional expression of an apparent splice variant of the murine 5-HT_3 receptor A subunit. *Eur J Pharmacol* **245:**187–192.

Hope A, Peters J, Brown A, Lambert J, and Blackburn T (1996) Characterization of a human 5-hydroxytryptamine3 receptor type A (h5-HT3R-AS) subunit stably expressed in HEK 293 cells. *Br J Pharmacol* **118:**1237–1245.

Jenkinson D (1960) The antagonism between tubocurarine and substances which depolarize the motor end-plate. *J Physiol (Lond)* **152:**309–324.

Karnovsky A, Gotow L, McKinley D, Piechan J, Ruble C, Mills C, Schellin K, Slightom J, Fitzgerald L, Benjamin C, et al. (2003) A cluster of novel serotonin receptor 3-like genes on human chromosome 3. *Gene* **319:**137–148.

Kelley S, Dunlop J, Kirkness E, Lambert J, and Peters J (2003) A cytoplasmic region determines single-channel conductance in 5-HT_3 receptors. *Nature (Lond)* **424:**321–324.

Ku H (1966) Notes on the use of propagation of error formulas. *J Res Nat Bur Standards C Eng Instrum* **70C:**263–273.

Lester H, Dibas M, Dahan D, Leite J, and Dougherty D (2004) Cys-loop receptors: new twists and turns. *Trends Neurosci* **27:**329–336.

Lummis S, Kilpatrick G, and Martin I (1990) Characterization of 5-HT_3 receptors in intact N1E-115 neuroblastoma cells. *Eur J Pharmacol* **189:**223–227.

Maksay G, Bikadi Z, and Simonyi M (2003) Binding interactions of antagonists with 5-hydroxytryptamine$_{3A}$ receptor models. *J Recept Signal Transduct Res* **23:**255–270.

Malany S, Osaka H, Sine S, and Taylor P (2000) Orientation of α-neurotoxin at the subunit interfaces of the nicotinic acetylcholine receptor. *Biochemistry* **39:**15388–15398.

Morales M and Wang S (2002) Differential composition of 5-hydroxytryptamine$_3$ receptors synthesized in rat CNS and peripheral nervous system. *J Neurosci* **22:**6732–6741.

Morris G, Goodsell D, RS H, Huey R, Hart W, Belew R, and Olson A (1998) Automated docking using Lamarckian genetic algorithm and an empirical free energy binding free energy function. *J Comp Chem* **19:**1639–1662.

Newberry N, Cheshire S, and Gilbert M (1991) Evidence that the 5-HT_3 receptors of the rat, mouse, and guinea-pig superior cervical ganglion may be different. *Br J Pharmacol* **102:**615–620.

Osterberg F, Morris G, Sanner M, Olson A, and Goodsell D (2002) Automated docking to multiple target structures: incorporation of protein mobility and structural water heterogeneity in AutoDock. *Prot Struct Func Genet* **46:**34–40.

Papineni R and Pedersen S (1997) Interaction of. *d*-tubocurarine with the mouse nicotinic acetylcholine receptor: ligand orientation at the binding site. *J Biol Chem* **272:**24891–24898.

Pedersen S and Papineni R (1995) Interaction of *d*-tubocurarine analogs with the *Torpedo* nicotinic acetylcholine receptor. Methylation and stereoisomerization affect site-selective competitive binding and binding to the noncompetitive site. *J Biol Chem* **270:**31141–31150.

Peters J, Malone H, and Lambert J (1990) Antagonism of $5HT_3$ receptor-mediated currents in murine N1E-115 neuroblastoma cells by (+)-tubocurarine. *Neurosci Lett* **110:**107–112.

Pettersen E, Goddard T, Huang C, Couch G, Greenblatt D, Meng E, and Ferrin T (2004) UCSF Chimera: a visualization system for exploratory research and analysis. *J Comput Chem* **25:**1605–1612.

Reeves D and Lummis S (2002) The molecular basis of the structure and function of the 5-HT_3 receptor: a model ligand-gated ion channel. *Mol Membr Biol* **19:**11–26.

Reeves D, Sayed M, Chau P-L, Price K, and Lummis S (2003) Prediction of 5-HT_3

receptor agonist-binding residues using homology modeling. *Biophys J* **84:**2338–2344.
Sali A and Blundell T (1993) Comparative protein modeling by satisfaction of spatial restraints. *J Mol Biol* **234:**779–815.
Smit A, Syed N, Schaap D, van Minnen J, Klumperman J, Kits KS, Lodder H, van der Schors R, van Elk R, Sorgedrager B, et al. (2001) A glia-derived acetylcholine-binding protein that modulates synaptic transmission. *Nature (Lond)* **411:**261–268.
Thompson A, Price K, Reeves D, Chan S, Chau P, and Lummis S (2005) Locating an antagonist in the 5-HT_{3R} receptor binding site using modeling and radioligand binding. *J Biol Chem* **280:**20476–20482.
Willcockson I, Hong A, Whisenant R, Edwards J, Wang H, Sarkar H, and Pedersen S (2002) Orientation of *d*-tubocurarine in the muscle nicotinic acetylcholine receptor-binding site. *J Biol Chem* **277:**42249–42258.
Yan D, Pedersen S, and White M (1998) Interaction of D-tubocurarine analogs with the $5HT_3$ receptor. *Neuropharmacology* **37:**251–257.
Yan D, Schulte M, Bloom K, and White M (1999) Structural features of the ligand-binding domain of the serotonin $5HT_3$ receptor. *J Biol Chem* **274:**5537–5541.
Yan D and White M (2002) Interaction of *d*-tubocurarine analogs with mutant 5-HT_3 receptors. *Neuropharmacology* **43:**367–373.
Yan D and White M (2005) Spatial orientation of the antagonist granisetron in the ligand-binding domain of the 5-HT_3 receptor. *Mol Pharmacol* **68:**365–371.
Yang J, Mathie A, and Hille B (1992) 5-HT_3 receptor channels in dissociated rat superior cervical ganglion neurons. *J Physiol (Lond)* **448:**237–256.
Zamyatnin A (1984) Amino acid, peptide, and protein volume in solution. *Annu Rev Biophys Bioeng* **13:**145–165.

Address correspondence to: Dr. Michael M. White, Department of Pharmacology and Physiology, Drexel University College of Medicine, 245 N. 15th Street, Philadelphia, PA 19102. E-mail: mikewhite@drexel.edu